Traffic 2000 1: 480–493
Munksgaard International Publishers

ISSN 1398-9219

Apical and Basolateral Endocytic Pathways of MDCK Cells Meet in Acidic Common Endosomes Distinct from a Nearly-Neutral Apical Recycling Endosome

Exing Wang[a], Paul S. Brown[a], Benjamin Aroeti[c], Steven J. Chapin[b], Keith E. Mostov[b] and Kenneth W. Dunn[a]*

[a] *Department of Medicine, Indiana University School of Medicine, 1120 South Drive, FH115, Indianapolis, IN 46202-5116, USA*
[b] *Department of Anatomy and Department of Biochemistry and Biophysics, University of California, San Francisco, CA 94143-0452, USA*
[c] *Department of Cell and Animal Biology, The Hebrew University of Jerusalem, Givat Ram, Jerusalem, Israel*
** Corresponding author: K.W. Dunn, kwdunn@iupui.edu*

Quantitative confocal microscopic analyses of living, polarized MDCK cells demonstrate different pH profiles for apical and basolateral endocytic pathways, despite a rapid and extensive intersection between the two. Three-dimensional characterizations of ligand trafficking demonstrate that the apical and basolateral endocytic pathways share early, acidic compartments distributed throughout the medial regions of the cell. Polar sorting for both pathways occurs in these common endosomes as IgA is sorted from transferrin to alkaline transcytotic vesicles. While transferrin is directly recycled from the common endosomes, IgA is transported to a downstream apical compartment that is nearly neutral in pH. By several criteria this compartment appears to be equivalent to the previously described apical recycling endosome. The functional significance of the abrupt increase in lumenal pH that accompanies IgA sorting is not clear, as disrupting endosome acidification has no effect on polar sorting. These studies provide the first detailed characterizations of endosome acidification in intact polarized cells and clarify the relationship between the apical and basolateral endocytic itineraries of polarized MDCK cells. The extensive mixing of apical and basolateral pathways underscores the importance of endocytic sorting in maintaining the polarity of the plasma membrane of MDCK cells.

Key words: Acidification, endocytosis, endosome, epithelia, immunoglobulin A, MDCK, polarity, polymeric Ig receptor, transferrin, transcytosis

Received 10 January 2000, revised and accepted for publication 10 March 2000

Endosome acidification is a defining characteristic of endosomes that is crucial to a variety of cellular processes. Early studies determined that endosome acidification mediates the receptor–ligand dissociation required for efficient receptor recycling, iron transport via the carrier protein transferrin (Tf) and activation of lysosomal acid hydrolases [reviewed by Mellman et al. (1) and Mukherjee et al. (2)]. Recent studies have identified a role for endosome acidification in a variety of other cellular processes including regulating rates of membrane internalization and recycling (3,4), ligand delivery to late endosomes and lysosomes (4,5), transport from endosomes to the *trans*-Golgi network (6), regulated expression of GLUT4 transporters (7) and resensitization of the beta2-adrenergic receptor (8). In addition to these normal cellular processes, endosome acidification is also required for cytosolic penetration by certain enveloped viruses and bacterial toxins (2) and for the intracellular transport of certain drugs (9).

Endosome acidification has been most completely characterized for non-polarized cells, but its functions may be uniquely important to polarized epithelial cells. The role of endosome acidification in the transport of toxins, drugs and pathogens are particularly relevant since epithelia are generally the first cells exposed to exogenous materials and pathogens, frequently providing the portal for entry into the body. In addition, epithelial transcytosis is dependent upon endosome acidification. Agents known to alkalinize endosomes have been observed to stimulate basolateral-to-apical transcytosis in MDCK cells (10) and to inhibit apical-to-basolateral transcytosis of VSV-G protein (11).

The regulation of endosome pH by epithelial cells may also be fundamentally different from that described in non-polarized cells. Endosome acidification is accomplished through the pumping of protons by the vacuolar H^+-ATPase. However, endosome pH is partially determined by the activity of other ion transporters, including the Na^+/K^+-ATPase (12–14), various Cl^- channels (14–18) and the Na^+/H^+ exchanger 3 (19). Since various forms of each of these transporters are polarized to either the apical or basolateral plasma membrane domain of epithelial cells, the regulation of endosome acidification by epithelial cells may differ from that in non-polarized cells and may also differ between apical and basolateral endosomes.

Separate modulation of apical and basolateral endosome pH is possible only to the degree that the two populations of endosomes are distinct from one another. While early studies indicated separate populations of early endosomes in polarized MDCK cells (20,21), recent studies have detected compartments containing both apical and basolateral endocytic probes (22–25). Nonetheless, the relationship between the apical and basolateral pathways remains unclear, and the studies of Henkel et al. (26) indicate that apical endosome pH can be selectively altered. These studies showed that ex-

pression of the influenza M2 proton channel protein in polarized MDCK cells disrupted apical IgA delivery without affecting the pH-sensitive basolateral recycling of Tf.

Endosome pH regulation in epithelial cells has been addressed in studies of isolated endosome preparations of kidney proximal tubule (15,27) and liver (18,28,29) and in studies of intact epithelial cells grown on glass [e.g. (30,31)]. However, none of these studies were capable of separately addressing pH regulation for the apical and basolateral endocytic pathways. The development of methods for microscopy of living cells grown on permeable supports, combined with a confocal microscopic assay of endosome pH has allowed us to provide the first detailed characterizations of endosome acidification in intact polarized cells.

These studies demonstrate that endosomes on the basolateral recycling pathway are acidified to a pH of 5.8, while the

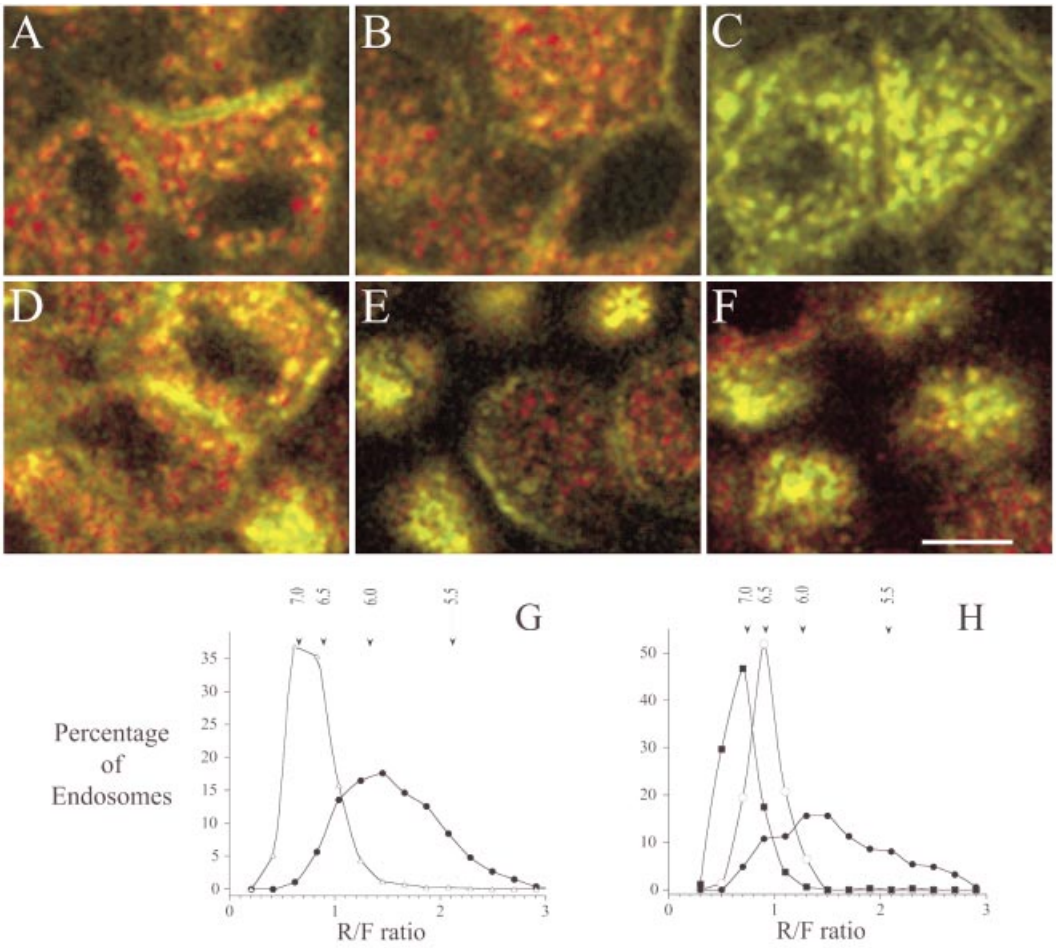

Figure 1: pH-sensitive endocytic ligands in living cells. A. A field of living polarized MDCK cells imaged in the presence of basolateral FR-Tf. B. As in A, but showing supranuclear planes of several cells. C. FR-Tf following collapse of endosomal pH gradients by addition of 40 mM methylamine. D. A field of living polarized MDCK cells imaged in the presence of basolateral FR-IgA. E, F. Supranuclear planes of several cells imaged in the presence of basolateral FR-IgA, showing alkaline apical endosomes of several cells as well as dim, acidic medial endosomes of other cells. G. Tf-containing endosomes are acidified to a pH of 5.8. Cells were incubated with FR-Tf for 20 min and imaged live in the continued presence of extracellular ligand. Histograms indicate the rhodamine-to-fluorescein ratios (R/F ratio) of individual endosomes before (circles, N = 1658) and approximately 5 min after addition of 1 μM bafilomycin (triangles, N = 685). Comparison of these distributions with calibration curves constructed with comparably labeled, fixed cells equilibrated with pH buffers indicates a mean endosome pH of 5.8, which increased to 6.7 after addition of bafilomycin. H. Basolaterally internalized IgA traverses endosomes regulated to two distinct pH values. Cells were incubated with FR-IgA for 20 min and imaged live in the continued presence of extracellular ligand. Images were collected at the apices or medial planes of cells at the level of the nuclei. Histograms indicate R/F ratios of medial compartments (closed circles, N = 200), apical endosomes (open circles, N = 77) and medial compartments following collapse of pH gradients with 40 mM methylamine (squares, N = 670). Comparison of these distributions with calibration curves indicates a mean pH of 5.7 for medial endosomes and a mean pH of 6.5 for AREs. Methylamine raised endosome pH to 7.2. Note that the relationship between R/F ratio and pH varies between experiments according to how probes are labeled with fluorophores and according to how the imaging detectors are configured. Scale bar represents 10 μm.

apical recycling pathway includes an early compartment with a pH of 5.8 and a later compartment, the apical recycling endosome (ARE), whose pH is 6.5. The similar pH of the early compartments of the apical and basolateral pathways reflects the fact that membrane probes internalized either apically or basolaterally are rapidly directed to the same set of acidic medial endosomes. In these acidic medial endosomes, IgA internalized from either plasma membrane domain is efficiently sorted from basolaterally recycling Tf and directed to the relatively alkaline ARE, prior to delivery to the apical plasma membrane. Although lumenal alkalinization occurs with the formation of transcytotic vesicles, the functional significance of the abrupt increase in lumenal pH that accompanies IgA sorting is not clear, as disrupting endosome acidification has no effect on polar sorting.

Results

The membrane endocytic pathways of MDCK cells were addressed using the PTR9 cell line, an MDCK clone transfected with the human transferrin receptor (TfR) and the rabbit polymeric Ig receptor (pIgR). The expression of the human TfR allows the use of Tf to characterize the basolateral recycling pathway. Since pIgR is both transcytosed from the basolateral plasma membrane to the apical plasma membrane, and recycled at the apical plasma membrane of transfected MDCK cells (32), the expression of pIgR allows the use of IgA to characterize the transcytotic and apical recycling pathways. Previous studies have demonstrated the appropriate behavior of the transfected TfR and pIgR in these cells (33).

Endosome acidification on the basolateral recycling pathway

To characterize acidification on the basolateral recycling pathway, PTR cells were incubated with Tf conjugated to fluorescein and rhodamine (FR-Tf). In order to provide steady-state imaging of endosomes despite rapid ligand flux, cells were labeled to steady state and then imaged in the presence of extracellular ligand, taking advantage of the narrow optical section provided by confocal microscopy. Confocal microscopic images of living, polarized PTR cells show that FR-Tf is internalized into endosomes both around and above the nuclei (Figure 1A,B). Since fluorescein's fluorescence is quenched at acidic pH, the fluorescence of FR-Tf internalized into acidic endosomes appears orange, while that bound to the plasma membrane appears green, reflecting the neutral pH of the extracellular medium. When transmembrane pH gradients are collapsed by the addition

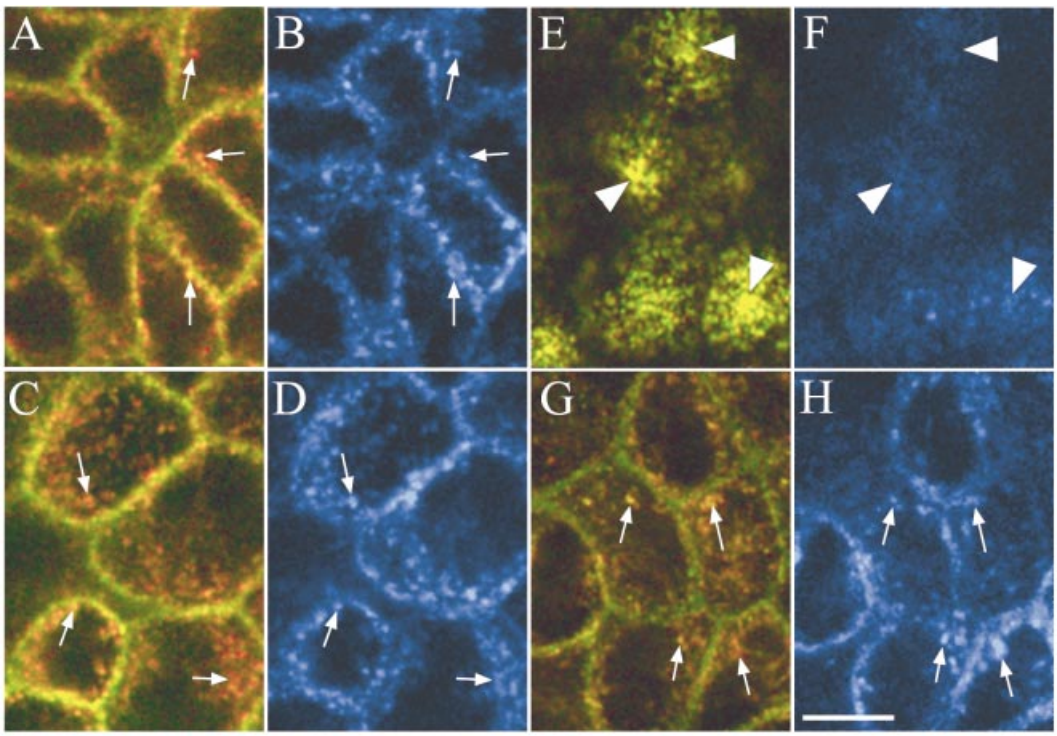

Figure 2: IgA is delivered to acidic compartments containing Tf prior to sorting to relatively alkaline compartments lacking Tf. Living, polarized cells imaged within 4 min of basolateral exposure to FR-IgA and Cy5-Tf, respectively, show IgA colocal with Tf in uniformly acidic compartments (A and B). Similar observations are made for cells imaged within 11 min of exposure to FR-IgA and Cy5-Tf, respectively (C and D). After 50 min exposure to FR-IgA and Cy5-Tf, apical focal planes show IgA in alkaline compartments lacking Tf (E and F). Medial focal plane of the same field shown in E and F shows IgA and Tf colocal in acidic medial compartments (G and H). Arrows indicate medial endosomes containing both Tf and IgA, arrowheads indicate apical endosomes enriched in IgA, but lacking Tf. Scale bar represents 15 μm.

of the weak base methylamine, endosomes alkalinize and the endosomal fluorescein fluorescence increases to levels equivalent to that at the plasma membrane (Figure 1C).

The pH of individual endosomes was quantified using a previously described ratiometric method in which the pH-independent fluorescence of rhodamine is divided by the pH-sensitive fluorescence of fluorescein (R/F ratio) (4,30,34). This ratio is sensitive to pH, but independent of the amount of ligand in an endosome or its focal position. The results of these quantifications are presented as histograms in Figure 1G. Comparisons of these ratios with pH standards indicate a mean pH of 5.8 for Tf-containing endosomes. Similar to previous studies (3,35,36), endosome acidification is partially sensitive to bafilomycin, which increases endosome pH to 6.7 within approximately 5 min of addition. Subsequent addition of the weak base methylamine equilibrates endosome pH with that of the medium.

The recycling pathway of some fibroblasts consists of an acidic sorting endosome, where recycling ligands are sorted from lysosomally directed ligands, and a relatively alkaline recycling endosome, where receptors are directed prior to return to the plasma membrane (3,12,37,38). While the endocytic itinerary of Tf in MDCK cells likewise consists of an early sorting endosome and a later recycling compartment (33), neither the fluorescence images nor the histograms indicate an alkaline pH for the recycling endosomes of MDCK cells. In order to separately measure the pH of sorting endosomes and recycling endosomes, cells were incubated with FR-Tf and diD-LDL [a far-red fluorescing form of LDL (33)]. Although the recycling endosomes of MDCK cells are not morphologically distinct, they can nonetheless be distinguished from sorting endosomes by the lack of LDL (33). Using LDL to identify sorting endosomes, this analysis detected no difference in the pH of sorting and recycling endosomes (data not shown).

Endosome acidification on the basolateral transcytotic pathway

The pH of endosomes on the transcytotic pathway of MDCK cells was addressed by imaging cells incubated with IgA conjugated to both fluorescein and rhodamine (FR-IgA) from the basolateral side of polarized monolayers. In contrast to the recycling pathway labeled with Tf, the transcytotic pathway labeled with basolateral FR-IgA includes two distinct lumenal pH environments. While endosomes in medial planes are highly acidified, condensed endosomes at the apices of the cells are more alkaline. Figure 1D–F show fields of cells incubating in FR-IgA. Depending upon the height of a particular cell, the focal plane passes through the medial region of the cell, which contains orange (acidic) endosomes, or through the apical region, containing green (more alkaline) endosomes. Figure 1D contains primarily medial endosomes, with the bright apical region of one cell shown at bottom right. The relative brightness of the apical and medial endosomes can be better appreciated when images are collected so that the images of apical endosome fluorescence are not saturated, in which case the acidic, medial endosomes appear very dim (Figure 1E,F).

R/F ratios of cells incubating in FR-IgA were calculated for both medial (at the level of the nuclei) and apical endosomes and are shown in Figure 1H. Comparisons with calibration pH standards indicate that the mean pH of medial endosomes is 5.7 (closed circles) while that of condensed apical compart-

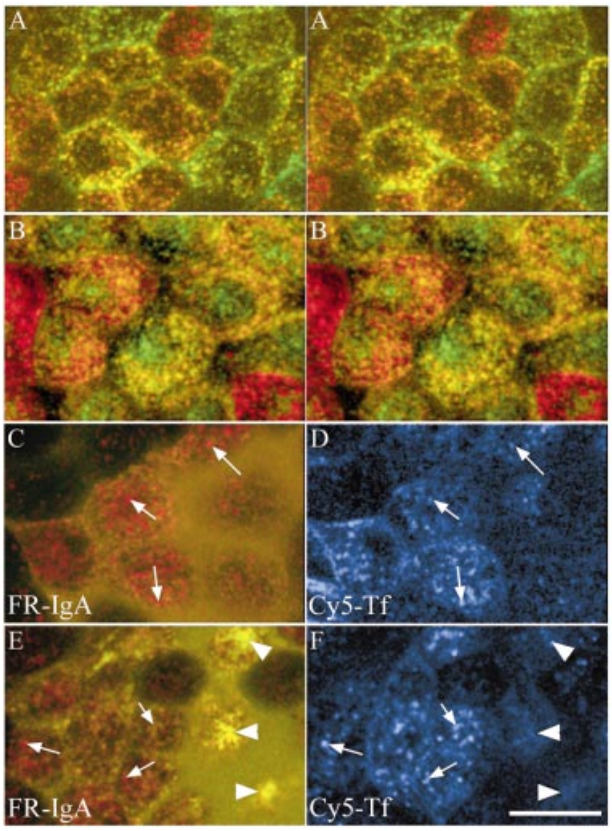

Figure 3: IgA internalized either basolaterally or apically is directed first to medial endosomes containing Tf, prior to sorting to apical compartments lacking Tf. A. Stereopair projections of cells fixed after incubation with TxR-Tf (red) and OG-IgA (green) for 5 min show that Tf and IgA are extensively colocal in medial endosomes. B. Stereopair projections of cells fixed after incubation with OG-IgA and TxR-Tf for 15 min show that by 15 min, while the two probes are still colocal in medial endosomes, much of the IgA is now sorted to apical compartments lacking Tf. Note that these stereopairs are also presented as movies of rotated projections in the Photo Gallery at www.traffic.dk. C–F. Apically internalized IgA is rapidly delivered to acidic, Tf-containing compartments prior to delivery to nearly-neutral AREs lacking Tf. Polarized cells imaged in the presence of apical FR-IgA and basolateral Cy5-Tf after 7 min of incubation show IgA in uniformly acidic compartments, most of which contain basolaterally internalized Tf (C and D, respectively). Polarized cells imaged in the presence of apical FR-IgA and basolateral Cy5-Tf after 40 min of incubation show IgA in acidic medial endosomes, most of which contain Tf, but also in alkaline apical compartments lacking Tf (E and F, respectively). Arrows indicate examples of endosomes containing both Tf and IgA, arrowheads indicate apical compartments lacking Tf. Scale bar represents 15 μm.

ments is 6.5 (open circles). Addition of methylamine raises endosome pH to 7.2 (squares). Although the apical compartments are located at the extreme apical pole of cells, their mildly acidic measured pH indicates that they are indeed intracellular endosomes, rather than an accumulation at the plasma membrane. This conclusion is also supported by studies demonstrating that the apical endosome is insensitive to apical trypsin (33) and inaccessible to apical antibodies (data not shown).

The distribution and pH of the acidic, IgA-containing compartments are similar to those of Tf-containing endosomes of the recycling pathway suggesting that IgA may traverse acidic, Tf-containing endosomes prior to delivery to the apical compartment. This conclusion is supported by studies in which cells were imaged at various times after addition of FR-IgA and Cy5-Tf. After 4 min of incubation, endosomal IgA is limited to acidic, medial endosomes that also contain Tf (Figure 2A,B). Similar results are found after 11 min of incubation (Figure 2C,D). However, after protracted incubations, IgA is also found in alkaline apical compartments lacking Tf (Figure 2E,F). Images of circumnuclear planes of the same cells (Figure 2G,H) show that Tf and IgA are widely colocal in the relatively dim, acidic endosomes of the medial planes.

These results agree with recent studies demonstrating that IgA is sorted from Tf in medial endosomes prior to delivery to

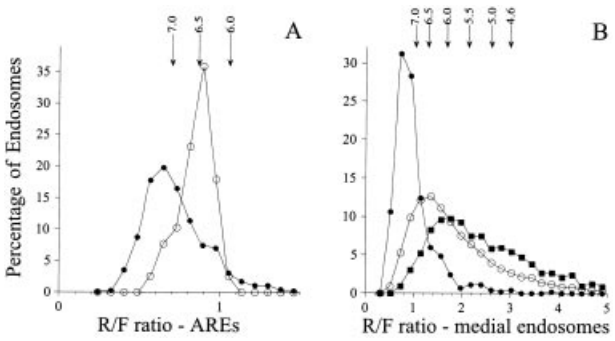

Figure 4: Apically internalized IgA is delivered to compartments with the same pH as those containing basolaterally internalized IgA. Cells were incubated with FR-IgA for 30 min and imaged live in the continued presence of extracellular ligand. Images were collected from either apical or circumnuclear planes for quantification of ARE and medial endosomes, respectively. A. R/F ratios of AREs (open circles, N = 39) and of endosomes in cells treated with 40 mM methylamine (closed circles, N = 463). Comparison of these distributions with calibrated fixed samples indicates a mean endosome pH of 6.5 for AREs and a mean pH of 6.9 for endosomes following methylamine treatment. B. R/F ratios of endosomes of medial planes of control cells (open circles, N = 15990) and of cells treated with 40 mM methylamine (closed circles (N = 452). Squares indicate the R/F ratios of cells that had been previously treated with 33 μM nocodazole at 37° for 1 h, then incubated with apical FR-IgA for 60 min in the continued presence of nocodazole (N = 1303). Comparisons with calibrated fixed samples indicates a mean pH of 5.8 for medial endosomes, a mean pH of 5.2 for endosomes of nocodazole-treated cells and a pH of 7.1 for endosomes following methylamine treatment.

an apical endocytic compartment (33). Although apparent in the images of living cells shown in Figure 2, this sorting itinerary is clearer in the three-dimensional images of fixed cells shown in Figure 3 (also reproduced as rotating projections in the Photo Gallery at www.traffic.dk). After 5 min of internalization, Texas Red-Tf (TxR-Tf) and Oregon Green-IgA (OG-IgA) closely colocalize in endosomes distributed throughout the cells (Figure 3A). With subsequent incubation, an accumulation of compartments containing IgA alone appears at the extreme apex of each cell (Figure 3B). Data presented elsewhere (33) demonstrate that by a variety of criteria, this apical compartment is equivalent to the apical recycling endosome (ARE) described by Apodaca et al. (22) and Barroso and Sztul (23). Taken together, these data demonstrate that basolaterally internalized IgA and Tf share an acidic compartment from which IgA is sorted to the relatively alkaline ARE.

Endosome acidification on the apical recycling pathway

Previous studies have demonstrated that the apical recycling and transcytotic pathways intersect in the ARE (22,23). The relatively alkaline pH of the ARE raised the possibility that the apical recycling pathway might be regulated to a higher pH than that of the basolateral recycling pathway. Since a significant fraction of pIgR is transcytosed to the apical plasma membrane where it recycles (32), we addressed acidification on the apical recycling pathway by incubating cells with FR-IgA from the apical side of the monolayer.

Surprisingly, apically internalized IgA shows the same acidification itinerary as basolaterally internalized IgA. Figure 3C shows a field of cells imaged in the presence of apical FR-IgA after 6 min of exposure. In this tilted optical section, which transects medial planes of the cells on the left of the field and apical planes of cells on the right, all endosomes are acidic, and there is no evidence of an apical compartment. When the duration of uptake is extended to 40 min (Figure 3E), a similar field of cells clearly shows both acidic medial endosomes (red) as well as alkaline apical endosomes (green). The hazy green fluorescence surrounding the tops of the cells on the right side of each field reflects the fluorescence of FR-IgA in the neutral apical medium.

The pH of endosomes on the apical recycling pathway was measured by incubating cells to steady state with apical FR-IgA and then calculating R/F ratios for both AREs and medial endosomes. As was previously found using basolaterally internalized IgA, R/F ratios for AREs measured using apically internalized IgA indicate a pH of 6.5 (Figure 4A). R/F ratios for medial endosomes labeled with apical FR-IgA indicate a pH of 5.8, nearly identical to that measured using basolaterally internalized IgA (Figure 4B).

Intersection between the apical and basolateral membrane pathways

The reason for the similarity of the acidification pathways followed by apically or basolaterally internalized IgA is indicated by comparison of the companion images of basolaterally internalized Cy5-Tf collected along with the images of

apically internalized FR-IgA shown in Figure 3. These figures show that the itinerary of apical IgA is similar to that of IgA internalized basolaterally. The image of Cy5-Tf shown in Figure 3D shows that most of the acidic, medial compartments to which apical FR-IgA is directed within 6 min of internalization appear to also contain Tf (some of which are indicated with arrows). The apical compartments to which apical IgA is directed with subsequent incubation (arrowheads in Figure 3E,F) become intensely labeled with IgA, but are depleted of Tf. Thus, like basolateral IgA, apical IgA is rapidly directed to acidic endosomes containing Tf, from which it is sorted to AREs lacking Tf.

These results indicate a significant overlap between the apical and basolateral recycling membrane pathways. To more accurately and completely assess this question, we conducted studies of fixed cells to characterize the three-dimensional distribution of apically and basolaterally internalized ligands. Figure 5 shows the results of an experiment in which cells were labeled for 15 min with basolateral TxR-Tf, basolateral OG-IgA and apical Cy5-IgA. Since interpretation of 3-color images is difficult, the different colors of fluorescence are presented two at a time. Figure 5A shows the combination of basolateral TxR-Tf and apical Cy5-IgA, while Figure 5B shows the combination of basolateral OG-IgA and apical Cy5-IgA.

The color stereopair in Figure 5A shows that apically internalized Cy5-IgA (pseudocolored green in this image) colocalizes with basolaterally internalized TxR-Tf (red) in medial endosomes, appearing yellow or orange. However, apically internalized IgA also accumulates in AREs lacking Tf, which thus appear green in these images. The similar itineraries of apical and basolateral IgA are evident in Figure 5B, which shows nearly identical endosomal distributions of IgA internalized apically (green) and basolaterally (red) in this same field of cells. The colocalization of the two probes in both medial compartments and the ARE is reflected by the constant yellow color of the endosomes in each cell. These images clearly show that apical IgA accesses medial endosomes containing basolaterally internalized Tf and IgA and, like basolateral IgA, is enriched relative to Tf in the ARE.

The relative distributions of apical and basolateral probes are more apparent in the single focal sections of this field shown in Figure 6 which show images of TxR-Tf, basolateral OG-IgA and apical Cy5-IgA in an apical plane (Figure 6A–C, respectively) and in a medial plane (Figure 6D–F). Like basolateral IgA (Figure 6B), apical IgA (Figure 6C) strongly labels the ARE, which is depleted in Tf (Figure 6A). However, in the medial planes shown in Figure 6D–F, it can be seen that apical IgA (Figure 6F), like basolateral IgA (Figure 6E), shares medial endosomes with Tf (Figure 6D).

The extent to which the apical and basolateral recycling pathways intermix is clearest in the high magnification images of a medial plane of living cells shown in Figure 6G,H. These figures show a striking colocalization of Tf and apically internalized IgA in both vesicles and what appear to be elaborate tubules even down to the level of the cell nucleus.

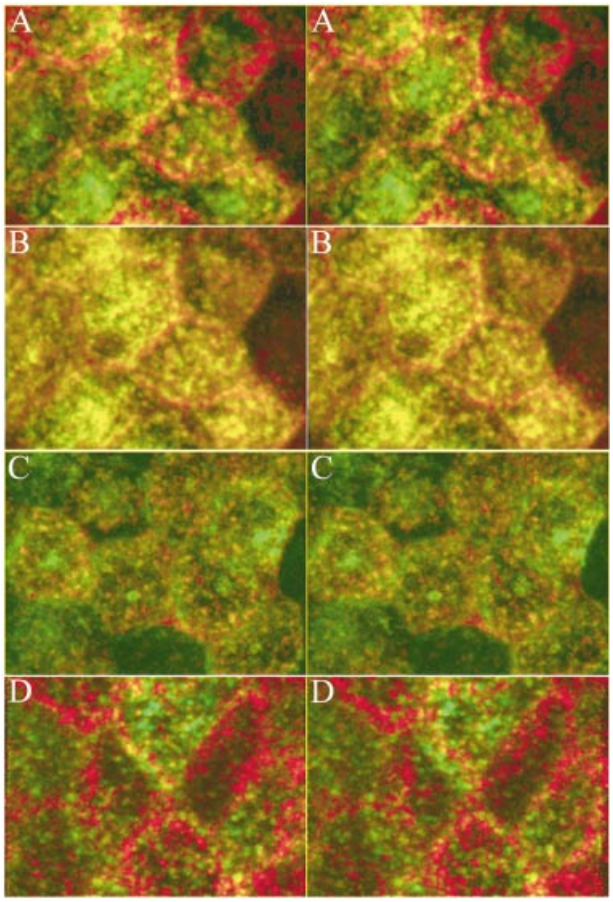

Figure 5: Three dimensional distributions of apically internalized IgA and basolaterally internalized Tf and IgA. A. Stereopair projection showing distribution of apically internalized Cy5-IgA (pseudocolored green) and basolaterally internalized TxR-Tf (red). IgA and Tf are colocal in medial endosomes, while IgA is enriched in apical endosomes lacking Tf. B. Stereopair projection of the same field as A, but showing combination of apically internalized Cy5-IgA (pseudocolored green) and basolaterally internalized OG-IgA (pseudocolored red). The two probes are extensively proportionally colocal in endosomes throughout the cell. C. Stereopair of cells labeled for 15 min with basolateral OG-IgA (green), with apical Cy5-IgA (red) included for the last 5 min. At this early time point, apical IgA has labeled medial endosomes containing basolateral IgA, but has not yet reached the ARE, which contains basolateral IgA alone. D. Stereopair projection of cells treated for 60 min incubation with 33 μM nocodazole then labeled for 30 min with apical Alexa488-IgA (green) and basolateral TxR-IgA (red) in the continued presence of nocodazole. Microtubule depolymerization locks IgA to regions adjacent to the plasma membrane domain from which it is internalized. Note that these stereopairs are also represented as movies of rotated projections in the Photo Gallery at www.traffic.dk. Scale bars were omitted from this figure as they interfere with stereo image formation. Panels A, B and D are 27 μm in height, C is 40 μm in height.

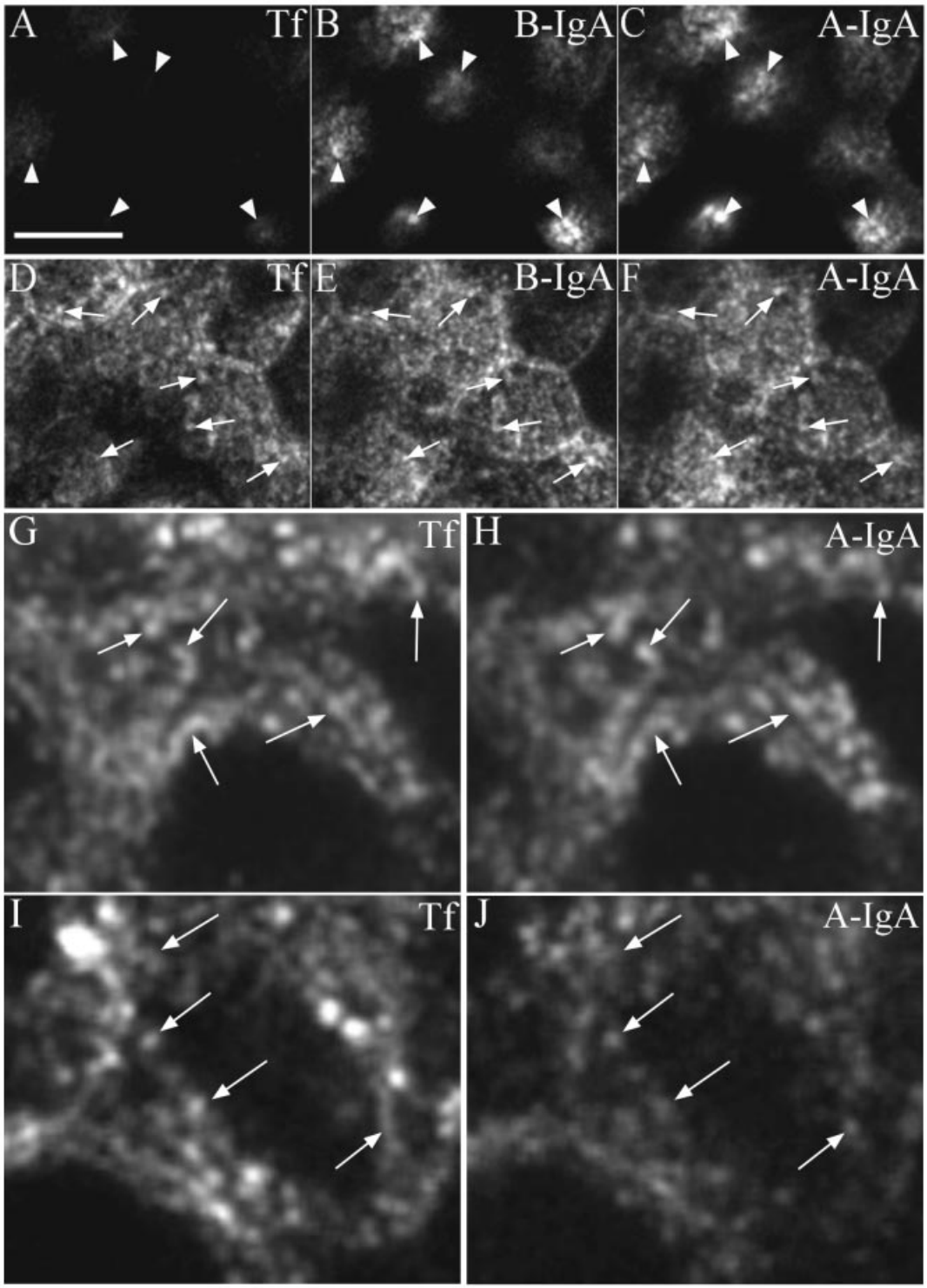

Figure 6: Pathway of apically internalized IgA. A, B and C show apical optical sections of cells incubated for 15 min with basolateral TxR-Tf, basolateral OG-IgA and apical Cy5-IgA, respectively. A corresponding optical section collected 2.4 μm lower is shown in panels D, E and F. This same field is depicted in the color stereopair projections shown in Figure 5, panels A and B. These images show that all three probes are extensively colocalized in medial planes, but Tf is depleted in the AREs that are enriched in apically and basolaterally internalized IgA. G, H. Higher magnification images of a medial plane of living cells show extensive colocalization of basolateral TxR-Tf and apical Alexa488-IgA in tubular endosomes even down to the level of the nuclei. I and J. High magnification images of cells incubated with basolateral TxR-Tf for 15 min with apical Alexa488-IgA included for the final 5 min. This image, collected in a medial plane located 8 μm below the apical surface shows how rapidly apical IgA accesses the basolateral recycling pathway as labeled with Tf. Arrowheads indicate the locations of AREs, and arrows indicate some especially clear examples of colocalization of Tf with apically internalized IgA. Scale bar represents 10 μm in panels A–F and 2.5 μm in panels G–J.

The speed with which apically internalized IgA accesses medial endosomes of the basolateral pathway is indicated in experiments in which cells were incubated with basolateral OG-IgA for 15 min, with apical TxR-IgA included for only the final 5 min. In the color stereopair shown in Figure 5C, medial endosomes appear orange, reflecting extensive colocalization of apically internalized TxR-IgA (red) with basolaterally internalized OG-IgA (green) in medial endosomes. At this early time point, however, apically internalized IgA has not yet reached the AREs, which appear green due to the presence of basolateral OG-IgA alone. These images demonstrate that apically internalized IgA rapidly accesses the medial endosomes of the basolateral pathway prior to delivery to the ARE.

In Figure 5C, one will also notice that the 5-min pulse of apical IgA has failed to reach endosomes at the base of each cell (appearing green). Nonetheless, even after this brief incubation, apical IgA can be detected in medial endosomes far from the apical surface. Figure 6I,J show an example of a focal plane collected 8 μm below the apical surface of a cell, in which apical IgA is beginning to label circumnuclear endosomes containing Tf. That apical IgA accesses Tf-containing endosomes at such depths after only 5 min of internalization emphasizes the speed and extent of access of apical IgA to the basolateral recycling pathway.

The interpretation that the similar acidification found for apical and basolateral endocytic pathways reflects mixing of the two is supported by studies showing that this similarity is

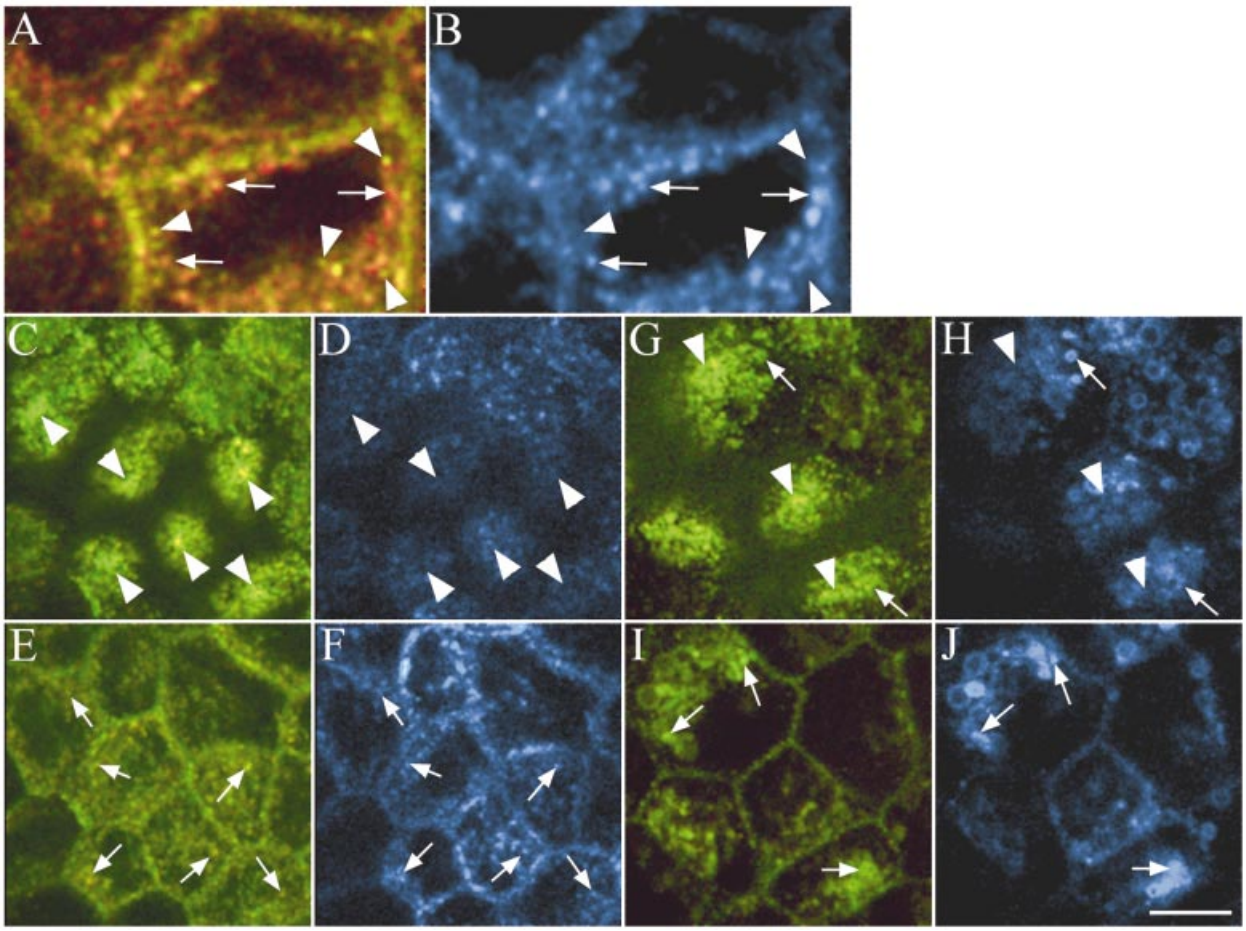

Figure 7: A sharp increase in pH accompanies sorting IgA into transcytotic vesicles, but endosome acidification is not necessary for polarized sorting. A, B. Image collected in a medial plane of living, polarized cells incubated with FR-IgA (E) and Cy5-Tf (F) for 10 min shows punctate compartments lacking Tf. These compartments, found far from the ARE, can be functionally defined as transcytotic vesicles. Transcytotic vesicles consistently show a strikingly higher pH than the endosomes containing both Tf and IgA. Panels C–F. Cells were treated with 1 μM bafilomycin for 20 min, then incubated with FR-IgA (shown in C and E) and Cy5-Tf (shown in D and F) for 20 min in the continued presence of bafilomycin. Images were then collected in the presence of drug and extracellular ligands at both the apex (panels C and D) or in a medial plane (panels E and F). As with untreated cells, IgA is efficiently sorted to AREs lacking Tf, despite endosome alkalinization. Panels G–J. Cells were treated with 40 mM methylamine for 5 min, then incubated with FR-IgA (shown in G and I) and Cy5-Tf (shown in H and J) for 20 min in the continued presence of methylamine. Images were then collected in the presence of drug and extracellular ligands at both the apex (panels G and H) or in a medial plane (panels I and J). Again IgA is efficiently sorted to AREs lacking Tf, despite endosome alkalinization. Arrows indicate endosomes containing both Tf and IgA, while arrowheads indicate AREs of the same cells that are enriched in IgA but lack Tf. Scale bar represents 10 μm.

sensitive to a manipulation that blocks mixing of apical and basolateral endocytic pathways. Consistent with previous studies (e.g. (22,23)), intermixing of the apical and basolateral endocytic pathways depends upon the presence of intact microtubules. Figure 5D shows that, following microtubule depolymerization by prior treatment with nocodazole, apical IgA (green) is limited to the cell apex, while basolateral IgA (red) is limited to the basolateral membranes. Measurements of the pH of these endosomes (shown in Figure 4B) indicate that microtubule depolymerization decreases the pH of endosomes containing apically internalized IgA to a mean of 5.2. These results suggest that IgA may pass through very acidic early apical endosomes prior to delivery to the medial common endosomes. We were unable to distinguish such compartments in studies in which endosome pH was measured following brief exposures to apical IgA (data not shown).

These data indicate that the similar pH found for apically recycling and basolaterally transcytotic IgA reflects the fact that the two are rapidly directed to the same pathway, consistent with previous studies (22). However, our results extend these studies, in that we find that the apical and basolateral recycling pathways do not intersect at the ARE, but rather in medial compartments preceding the ARE. Following apical internalization, IgA is rapidly directed to medial endosomes containing basolaterally internalized Tf, from which it is sorted to the ARE.

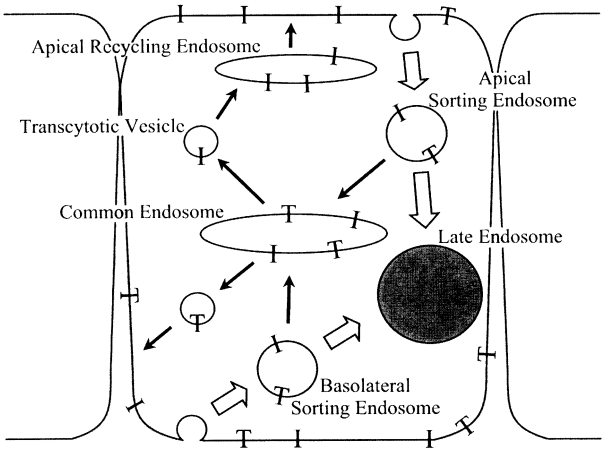

Figure 8: Schematic diagram of the endocytic pathways of polarized MDCK cells. Ligands bind to receptors at each plasma membrane from which they are internalized into distinct apical and basolateral sorting endosomes. Endosome acidification mediates dissociation of lysosomally directed ligands, which are directed to a set of late endosomes, where fluid-phase probes internalized from either plasma membrane domain intermix. Membrane proteins, in this case TfR (T) and pIgR (I) are sorted from apical and basolateral sorting endosomes to common endosomes. The common endosomes conduct polar sorting of membrane proteins internalized from either plasma membrane domain, sorting TfR to the basolateral plasma membrane and sorting pIgR into transcytotic vesicles that transport pIgR to the ARE prior to delivery to the apical plasma membrane. Although predominately a basolateral protein, TfR is also shown on the apical plasma membrane to demonstrate the capacity of the common endosome to correct protein mistargeting.

The role of endosome acidification in polar sorting

After 10–15 min of basolateral incubation with Tf and IgA, IgA appears alone not only in the ARE, but also in individual vesicles in medial planes. Many of these vesicles are found at the level of the nuclei several microns from the ARE. The medial localization of these sharply punctate vesicles, taken together with the fact that they appear only after an initial complete colocalization of IgA and Tf, suggests that these vesicles can be functionally identified as transcytotic vesicles. Surprisingly, we find that transcytotic vesicles, like the ARE, are relatively alkaline. Figure 7A,B show a circumnuclear plane of cells labeled for 20 min with FR-IgA and Cy5-Tf. Close comparison of the two images shows that compartments containing Tf (indicated with arrows) are consistently acidic (appearing red), while the punctate compartments lacking Tf (indicated with arrowheads) are consistently alkaline (appearing green).

The observation that sorting of IgA from Tf is accompanied by a significant increase in endosome pH suggested that the pH discontinuity between recycling endosomes and transcytotic vesicles may be involved in polarized sorting. This possibility was addressed by assessing IgA-Tf sorting in cells whose endosome acidification had been blocked with either bafilomycin or methylamine. Figure 7C–F show a field of living cells that had been exposed to 1 μM bafilomycin for 20 min prior to incubation with FR-IgA and Cy5-Tf in the continued presence of drug. Results presented above demonstrate that bafilomycin increases endosome pH to 6.7 within 5 min, an increase that is reflected in the constant green appearance of the FR-IgA-containing endosomes. Despite endosome alkalinization, IgA is efficiently sorted from Tf in these cells, as indicated by the delivery of IgA but not Tf to AREs. Similar to previous figures of untreated cells, bafilomycin-treated cells with equivalent amounts of Tf and IgA in medial endosomes (Figure 7E,F) show AREs in which IgA is enriched and Tf is depleted (Figure 7C,D).

Figure 7G–J show a field of living cells that had been exposed to 40 mM methylamine for 5 min prior to incubation in FR-IgA and Cy5-Tf in the continued presence of methylamine. Endosome pH increases virtually instantaneously to 7.1–7.2 upon addition of methylamine. Although endosome morphology is profoundly disrupted by this treatment, efficient sorting of IgA from Tf is reflected by the enrichment of IgA and depletion of Tf in AREs (Figure 7G,H) in cells with equivalent amounts of Tf and IgA in medial endosomes (Figure 7I,J). Taken together, these studies demonstrate that endosome acidification is not required for efficient polarized sorting of IgA from Tf.

Discussion

Previous studies of MDCK cells (22–25) and Caco-2 (39,40) cells have described a compartment where apical and basolateral membrane probes intermix. Our microscopic analyses of living cells have distinguished two such compartments, the ARE and the medial endosomes, whose accessibility

depends upon the destination of the membrane probe. Membrane probes internalized either apically or basolaterally are rapidly directed to a set of acidic (pH = 5.8) medial endosomes that we will refer to as 'common endosomes', after Hughson and Hopkins (39). These common endosomes perform polar sorting for both the apical and basolateral membrane pathways so that Tf is directly recycled to the basolateral plasma membrane and IgA, internalized either apically or basolaterally, is directed to the ARE. Thus, while the common endosomes are accessible to apically and basolaterally recycling probes as well as transcytotic probes, the downstream ARE is accessible only to proteins targeted to the apical plasma membrane (e.g. transcytotic or apically recycling IgA).

The ARE is distinctive in its extreme apical localization, lack of Tf, enrichment of IgA and nearly neutral pH (6.5). The ARE appears to be physically distinct from the common endosomes, as we observe sharp discontinuities in both pH and ligand constitution that would require extraordinary gradients within a single continuous compartment. In many of the images presented here, acidic common endosomes are found in close proximity to the lower reaches of the relatively alkaline ARE and common endosomes with a low IgA/Tf ratio are seen immediately adjacent to AREs with a high IgA/Tf ratio.

The pH and time-series morphological analyses presented here clarify the relationship between the apical and basolateral endocytic pathways, and emphasize the speed and extent of intermixing of basolaterally recycling Tf, transcytotic IgA and apically recycling IgA in the medial common endosomes. The distributions of transcytotic and apically recycling IgA are nearly superimposable in both the early acidic common endosomes and later alkaline ARE, showing that the two pathways are intermixed nearly to the point of functional equivalence.

These results contrast with previous observations that fluid-phase probes internalized apically and basolaterally do not intermix in 'early endosomes' of MDCK cells, suggesting the presence of separate populations of apical and basolateral endosomes (20,21,41). Differences in the observed intermixing of apical and basolateral probes in early endosomes may reflect important differences in how fluid-phase and membrane probes are transported through sorting endosomes, the compartments to which membrane and lysosomally directed ligands are directed immediately after internalization. Consistent with previous studies of fibroblasts (42–44), recent studies of polarized MDCK cells (33) demonstrate that while ligands are retained in sorting endosomes, membrane probes rapidly course through to the common endosomes. To the degree that fluid-phase and membrane probes predominately label sorting endosomes and common endosomes, respectively, the earlier studies of MDCK cells labeled with fluid-phase probes may have primarily characterized apical and basolateral sorting endosomes, while the later studies employing membrane probes may have characterized the common compartments.

The apparently conflicting results can be reconciled with a model of endocytosis with distinct apical and basolateral sorting endosomes, and shared common compartments to which membrane proteins from either domain are directed. Consistent with this interpretation, while apically internalized IgA rapidly colocalizes with basolateral IgA or Tf, a distinct set of apical compartments is labeled following brief incubations with apical dextran (23). Thus, while the apical and basolateral endocytic pathways share the common compartments, the sorting endosomes are distinct for each pathway.

The resulting model of endocytosis in polarized MDCK cells is shown in Figure 8. Ligands and receptors are internalized from either plasma membrane domain into separate basolateral and apical sorting endosomes. The low pH of these endosomes mediates dissociation of certain ligands, such as LDL, from their receptors. Receptors, in this example, pIgR (I) and TfR (T) are then sorted from apical and basolateral sorting endosomes to common endosomes, while volume probes (such as dextran or released LDL) are directed to late endosomes, where apical and basolateral volume probes intermix (20,21,41). Polar sorting occurs in the common endosomes such that TfR is efficiently sorted to the basolateral plasma membrane, while pIgR is sorted into transcytotic vesicles that transport pIgR to the ARE prior to delivery to the apical plasma membrane. Insofar as the common endosome performs polarized sorting for both apical and basolateral pathways, a single sorting process accomplishes efficient apical and basolateral recycling, transcytosis and correction of mistargeted receptors.

The rapid intermixing of the apical and basolateral endocytic pathways presumably overwhelms any potential differences in endosome pH regulation that might derive from differences in the ion transporters present in the apical or basolateral membrane of MDCK cells (45). This intermixing may also explain our observation that endosome pH is not significantly affected by the development of membrane polarity (data not shown). However, when mixing is blocked by microtubule depolymerization, an especially acidic population of apical endosomes (pH = 5.2) is detected. To the degree that nocodazole blocks efflux of IgA from an early apical compartment, these endosomes might represent short-lived, very acidic compartments early in apical endocytosis. Although such acidic early endosomes were not obvious in our measurements of apical endosome pH, the speed of IgA transit through these compartments may be such that they represent a small fraction of the endosomes labeled to steady state. Direct comparisons of the pH of sorting endosomes and common endosomes detected no such acidic early compartment on the basolateral pathway.

We find that the increase in endosome pH on the transcytotic pathway occurs at the stage of transcytotic vesicle formation. Punctate transcytotic vesicles, containing IgA but not Tf, are observed in circumnuclear planes of polarized cells, several microns away from the ARE. Dual label studies

with pH-sensitive probes demonstrate a striking correlation in which common endosomes containing Tf and IgA are acidic, while the transcytotic vesicles containing IgA alone are alkaline. The potential function of the abrupt increase in lumenal pH that accompanies IgA sorting into transcytotic vesicles is not clear. Previous studies have demonstrated that endosome acidification is required for the formation of carrier vesicles for late endosome transport (5,46). Our data provide no evidence that endosome acidification, nor the difference in pH between common endosomes and transcytotic vesicles is important to sorting and transport of IgA to the ARE. Efficient sorting of IgA from Tf and delivery to the ARE was observed in cells whose endosome acidification was blocked with bafilomycin, or whose endosomes were neutralized with methylamine.

Although we find that transport to the ARE is independent of endosome acidification, recent studies indicate that transport to the apical plasma membrane is regulated by endosome acidification. Henkel et al. (47) observed that expression of the influenza M2 proton channel alkalinized endosomes and reduced rates of Tf recycling in HeLa cells. In contrast M2 expression in polarized MDCK cells had no effect on basolateral Tf recycling, but reduced the rates of transcytosis and apical recycling of IgA (26). Insofar as our results identify the ARE as the sole site of selective modulation of acidification for the apical but not basolateral endocytic pathways, they confirm the suggestion by these authors that acidification is critical to efficient transport through the ARE. Although the function of the ARE is unknown, evidence suggests a role in regulated apical membrane transport (48,49). Interestingly, the same second messengers that alter rates of endocytosis also affect endosome pH (14,15), raising the possibility that regulated transport through the ARE is mediated via its lumenal pH.

The pH-sensitive transport of the ARE is similar to that of the pericentriolar recycling compartment (PRC) of Chinese Hamster Ovary cell fibroblasts. Efflux of Tf from the PRC is slowed in cells whose endosome acidification is blocked with bafilomycin (3,35), and in endosome acidification mutants (50). The ARE has been previously likened to the fibroblast PRC, with which it shares many characteristics. Both compartments are terminal recycling compartments, clustered adjacent to centrioles via microtubules and have been associated with rab11 and rab17 (22,51–60). Furthermore, like the ARE, the PRC is modestly acidified to a pH of 6.4 and follows an earlier acidic compartment with a pH of 6.0 (38,50).

Despite these similarities, the PRC is fundamentally different from the ARE in that while the majority of Tf recycles through the PRC of fibroblasts (43,50), studies presented here and elsewhere (33) demonstrate that Tf is efficiently excluded from the ARE of MDCK cells. The exclusion of Tf from the ARE does not reflect a change in membrane sorting that accompanies the development of cell polarity as comparable sorting of IgA occurs in flat, glass-grown MDCK cells. While such cells seldom display a condensed ARE, IgA is sorted from Tf to alkaline, rab-11 associated downstream compartments equivalent to the ARE [(33); data not shown].

The polarized phenotype of epithelial cells reflects an active process in which newly synthesized proteins and lipids are specifically sorted and targeted to particular plasma membrane domains. Our studies demonstrate that endocytosis then repeatedly and extensively shuffles proteins from the apical and basolateral domains, emphasizing the importance of endocytic sorting in maintaining epithelial polarity. Since the simplest system to maintain plasma membrane polarity would seem to be to one with separate apical and basolateral endosomes, the existence of such an apparently costly system begs the question of the advantage of intermixing the two pathways. One possibility is that this mechanism provides for proofreading, correction of mislocalized plasma membrane proteins.

Materials and Methods

Cell lines

The PTR cells used in these studies are MDCK strain II cells transfected with both the human TfR and the rabbit pIgR. Previous studies (33) have demonstrated that 85% of the transfected human TfR is expressed on the basolateral membrane of these cells and that the kinetics of Tf recycling and pIgR transcytosis agree well with previously published values for the parental cells (22) and for another MDCK cell line transfected with the human TfR (25). ^{125}I-Tf binding was found to be 95% compatible with excess unlabeled Tf. The specificity of the pIgR was described previously for the parental cells (32).

Cell culture

PTR cells were grown in MEM (Life Technologies, Grand Island, NY) with 8% fetal bovine serum (FBS), 1% L-glutamine, streptomycin, and 0.05% hygromycin (Calbiochem, San Diego, CA). Cells were passed every 3–4 days and growth medium changed daily. New cultures of cells were thawed every 4–5 weeks. For fluorescence experiments, cells were plated at confluence on the bottoms of collagen-coated Millipore CM 12-mm filters and cultured for 4–5 days prior to experiments. Bottom-seeding was accomplished by creating a cup on the underside of the filter units by wrapping parafilm around the base of the filter unit. The filter units are inverted and cells seeded into this parafilm cup overnight. The following morning, the parafilm was removed, the filters removed to their normal orientation in 24-well dishes and the cells were then grown hanging from the filter. At this point, *trans*-epithelial resistance plateaued at 450 ohms cm^2 as measured with a Millipore Millicell ERS resistance meter. Development of cell polarity was also indicated by the increase in cell height to between 12 and 18 μm, development of tight junctions (as assessed by immunofluorescence detection of the tight junction protein zo-1), 85% basolateral distribution of the TfR, and by the minimal apical endocytosis of Tf. Monolayer impermeability was indicated by a variety of criteria (see below).

Cells labeled with fluorescent LDL were cultured in medium containing 8% lipoprotein-deficient medium to up-regulate the expression of the LDL receptor. Comparisons of the Tf or IgA labeling patterns of these cells with cells cultured in complete medium showed no effects on the morphology of endosomal compartments.

Antibodies and proteins

Purified dimeric IgA was kindly provided by Professor J.-P. Vaerman (Catholic University of Louvain, Brussels, Belgium). Human Tf was obtained from Sigma (St Louis, MO), iron loaded and purified by S300 column purification as described in (38). Human LDL was obtained from Biomedical Technologies (Stoughton, MA). Anti zo-1 antibody was obtained from the Developmental Hybridoma Bank (University of Iowa) and anti-fluorescein antibody was obtained from Molecular Probes (Eugene, OR). With the exception of Cyanine 5.18 succinimidyl ester (Cy5), which was obtained from Amersham (Arlington Heights, IL), all fluorescent probes were obtained from Molecular Probes. All other reagents were obtained from Sigma.

Fluorescent ligand preparation

Fluorescent conjugates of Tf and IgA were prepared from succinimidyl esters of various fluorophores according to manufacturer's instructions. Oregon green 488 (OG) was added to Tf in a ratio of 12:1, and to IgA in a ratio of 16:1. Alexa 488 was conjugated to either Tf or IgA using the product protocol provided by Molecular Probes. TxR was added to Tf in a ratio of 2:1 and to IgA in a ratio of 8:1. Fluorescein-ex (F) was added to Tf in a ratio of 8:1. Cy5 was conjugated to both Tf and IgA in a ratio of approximately 4:1. For pH-sensitive dyes, Tf was conjugated to both fluorescein and rhodamine (FR-Tf) in a ratio of 6:2:1. IgA was conjugated to fluorescein and rhodamine (FR-IgA) in a ratio of 15:5:1.

Fluorescent LDL was prepared as described in (61) with diD (1,1′-dioctadecyl-3,3,3′,3′-tetramethylindodicarbocyanine perchlorate), dialyzed against 150 mM NaCl with 0.01% EDTA, sterile filtered and stored under argon.

Labeling of cells with fluorescent ligands

For fluorescence labelings, cells were incubated at 37°C on a slide warmer in a humidified chamber for 15 min prior to addition of fluorescent ligands. All incubations were conducted in Medium 1 (150 mM NaCl, 20 mM HEPES, 1 mM $CaCl_2$, 5 mM KCl, 1 mM $MgCl_2$, 10 mM glucose pH 7.4). As described in each study, cells were labeled with 20 μg/ml fluorescent Tf, 20 μg/ml fluorescent LDL or 100 μg/ml fluorescent IgA. After incubations with fluorescence ligands, filters were rinsed briefly in phosphate buffered saline (PBS) at 4°C, then incubated in 4% paraformaldehyde in PBS (pH 6.5) for 5 min, then transferred to 4% paraformaldehyde in 100 mM NaB_4O_7 (pH 11.0) for 10 min. Filters were then rinsed in PBS.

The specificity of receptor-mediated uptake of fluorescent LDL, IgA and Tf was demonstrated by its inhibition by competition with excess unlabeled ligands. Fluorescent IgA and Tf were both found to efflux the cells with kinetics similar to those of the radiolabeled ligands. Dual labeling experiments showed the endosomal distributions of ligands conjugated to different fluorophores to be identical.

Valid comparisons of the endocytic pathways of apically and basolaterally internalized probes depend upon the polarity of uptake. For several reasons, we are confident that the monolayers used in these studies are tight and, thus, that ligands are internalized strictly via the plasma membrane domain to which they are applied. First, monolayer impermeability was indicated by the *trans*-epithelial resistance measured for each experimental filter. Second, differences between the endosomal distributions of apically and basolaterally internalized IgA show that apical IgA is not internalized via the same pathway as basolateral IgA (see Results). Third, when IgA is presented on both sides of a monolayer, the basolateral probe is evident on the basolateral plasma membrane and intercalated into the filter matrix while extracellular apical IgA labels the apical plasma membrane. Similarly, experiments in which anti-fluorescein antibody was added apically showed that apical fluorescence was rapidly quenched with no effect on the ligand present in the basolateral medium. Fourth, unlike IgA, when Tf is presented on both sides of a monolayer, internalization is almost exclusively limited to the basolateral probe. Finally, separate apical and basolateral uptake pathways are observed in cells whose microtubules have been depolymerized by prior treatment with 33 μM nocodazole for 60 min at 37°C (see Results).

The kinetics of endocytic labeling from the basolateral side were unaffected by the filter, as we found that the permeation rates of F-Tf and diI-LDL (the two extremes in size) through the filters are identical.

Microscopy

All experiments were conducted using a Bio-Rad MRC-1024 laser scanning confocal attachment mounted on Nikon Diaphot 200 or Nikon Eclipse 200 inverted microscope using a Nikon 60X, N.A. 1.2 water immersion objective or Nikon 100X N.A. 1.4 oil immersion objectives. Illumination is provided by a Krypton-Argon laser providing for fluorescence excitations at 488 nm, 568 nm and 647 nm, allowing collection of up to three images simultaneously. In some experiments, potential bleed-through of the green channel into the red channel, and of the red channel into the far-red channel required that images be collected sequentially, in which case no between-channel bleed-through was detected. Image volumes were collected by collecting a vertical series of images, each between 0.2 and 0.6 μm apart. Photomultiplier offsets were set such that background was slightly positive to guarantee signal linearity with fluorescence. Whenever possible signal saturation was avoided, and objects with saturated pixels were omitted from quantifications.

As mentioned previously, cells were grown on the underside of Millipore filter units. After removing the legs of the filter units, living or fixed cells were observed by placing the entire filter unit on two 50 μm tape spacers attached to the coverslip of a coverslip-bottomed 35 mm dish (Mattek, Ashland, MA) mounted on the stage of an inverted microscope. For live cell studies, incubations are conducted in medium 1 on the microscope stage, with basolateral ligands added to the filter cup, while apical ligands are added to the well of the coverslip-bottomed dish. Temperature is maintained by a Medical Systems PDMI-2 open perfusion chamber (Greenvale, NY). Fixed cells were imaged immediately after fixation in PBS containing 2% DABCO (Sigma) (using the water immersion objective) or after mounting in Prolong (Molecular Probes) (using the oil immersion objective).

Image processing for presentation

Image processing was conducted using Metamorph software (Universal Imaging, West Chester, PA). In order to minimize photobleaching, and phototoxicity in living cells, all fields were imaged with minimal averaging (1–4 frames). To compensate, all images were subsequently averaged spatially using a 3×3 low pass filter where necessary. Images shown in figures were contrast stretched to enhance the visibility of dim structures, and specific care was taken never to enhance the contrast in such a way that dim objects were deleted from an image. Different focal planes from the same field were contrast enhanced identically. Montages were assembled and annotated using Photoshop (Adobe, Mountain View, CA).

Fluorescence ratio quantifications

Distinction of individual endosomes and quantification of endosome fluorescence was conducted as previously described (62). For endosome fluorescence ratio calculations, the common non-zero pixels for

each endosome were determined and the fluorescence ratio within that region calculated. In general, images of endosomes were segmented automatically using image processing techniques, but when it was necessary to hand-select endosomes for quantification, we guaranteed that sampling was unbiased with respect to the measured ratio by using only one image of the image pair to identify clearly labeled and distinct endosomes for quantification. As much as possible, detector saturation was avoided during collection, but when pixel saturation occurred, objects with pixels within 10% of saturation (with a gray level of 230 or above in the original image) were removed from analysis. The methods used here are as described previously (3,34,63).

Endosome acidification measurements were conducted using a fluorescence ratio technique described previously (30). Cells were incubated for 20 min with FR-IgA or FR-Tf and imaged in the continued presence of extracellular ligand. For each endosome the amount of fluorescein and rhodamine fluorescence was quantified, and the ratio calculated by digital image analysis as described above. Estimates of endosome pH were derived from calibration curves established from parallel samples of cells that were fixed after incubation with FR-IgA or FR-Tf and equilibrated with a range of pH buffers. New calibrations are established for each experiment as the relationship between R/F ratio and pH varies between experiments according to how probes are labeled with fluorophores and according to how the imaging detectors are configured. For comparison of the pH of sorting endosomes and recycling compartments, cells were incubated with both FR-Tf and diD-LDL for 20 min and images of medial planes were collected. Cells with sufficient FR-Tf labeling to support quantification and sufficient LDL uptake to allow reliable identification of sorting endosomes were selected for analysis. For each cell several endosomes containing Tf and LDL (sorting endosomes) or containing Tf but no detectable LDL (tubular compartments) were identified and the R/F fluorescence ratio quantified for each. A similar approach was taken to compare the pH of FR-IgA-containing endosomes in the presence or absence of Tf. Measurements of the pH of IgA-containing endosomes in medial planes were conducted either by individually identifying endosomes from circumnuclear planes (Figure 1H) or by selecting fields that included primarily circumnuclear endosomes (Figure 4B). AREs were identified by their extreme apical location, condensed structure and intense labeling. In all cases, where particular endosomes were selected for quantification, selection was conducted using images with no color information.

Acknowledgments

We thank Sven van IJzendoorn for helpful suggestions in the preparation of this manuscript. This work was supported by N.I.H. grant R29DK51098 (K.D.), a fellowship from the American Heart Association, Indiana Affiliate, Inc. (E.W.), the Israel Science Foundation founded by the Israel Academy of Sciences and Humanities (B.A.), an American Cancer Society Fellowship PF3666 (S.C.) and N.I.H. grant RO1AI25144 (K.M.).

References

1. Mellman I, Fuchs R, Helenius A. Acidification of the endocytic and exocytic pathways. Annu Rev Biochem 1986;55: 663–700.
2. Mukherjee S, Ghosh RN, Maxfield FR. Endocytosis. Physiol Rev 1997;77: 759–803.
3. Johnson LS, Dunn KW, Pytowski B, McGraw TE. Endosome acidification and receptor trafficking: bafilomycin A1 slows receptor externalization by a mechanism involving the receptor's internalization motif. Mol Biol Cell 1993;4: 1251–1266.
4. van Weert AW, Dunn KW, Gueze HJ, Maxfield FR, Stoorvogel W. Transport from late endosomes to lysosomes, but not sorting of integral membrane proteins in endosomes, depends on the vacuolar proton pump. J Cell Biol 1995;130: 821–834.
5. Clague MJ, Urbe S, Aniento F, Gruenberg J. Vacuolar ATPase activity is required for endosomal carrier vesicle formation. J Biol Chem 1994;269: 21–24.
6. Reaves B, Banting G. Vacuolar ATPase inactivation blocks recycling to the *trans*-Golgi network from the plasma membrane. FEBS Lett 1994;345: 61–66.
7. Chinni SR, Shisheva A. Arrest of endosome acidification by bafilomycin A1 mimics insulin action on GLUT4 translocation in 3T3-L1 adipocytes. Biochem J 1999;339: 599–606.
8. Krueger KM, Daaka Y, Pitcher JA, Lefkowitz RJ. The role of sequestration in G protein-coupled receptor resensitization. Regulation of beta2-adrenergic receptor dephosphorylation by vesicular acidification. J Biol Chem 1997;272: 5–8.
9. Steinberg TH. Cellular transport of drugs. Clin Infect Dis 1994;19: 916–921.
10. Melby EL, Prydz K, Olsnes S, Sandvig K. Effect of monensin on ricin and fluid phase transport in polarized MDCK cells. J Cell Biochem 1991;47: 251–260.
11. Pesonen M, Simons K. Transepithelial transport of a viral membrane glycoprotein implanted into the apical plasma membrane of Madin–Darby canine kidney cells. II. Immunological quantitation. J Cell Biol 1983;97: 638–643.
12. Cain CC, Sipe DM, Murphy RF. Regulation of endocytic pH by the Na+, K+-ATPase in living cells. Proc Natl Acad Sci USA 1989;86: 544–548.
13. Fuchs R, Schmid S, Mellman I. A possible role for Na+, K+-ATPase in regulating ATP-dependent endosome acidification. Proc Natl Acad Sci USA 1989;86: 539–543.
14. Zen K, Biwersi J, Periasamy N, Verkman AS. Second messengers regulate endosomal acidification in Swiss 3T3 fibroblasts. J Cell Biol 1992;119: 99–110.
15. Bae HR, Verkman AS. Protein kinase A regulates chloride conductance in endocytic vesicles from proximal tubule. Nature 1990;348: 637–639.
16. Barasch J, Gershon MD, Nunez EA, Tamir H, al-Awqati Q. Thyrotropin induces the acidification of the secretory granules of parafollicular cells by increasing the chloride conductance of the granular membrane. J Cell Biol 1988;107: 2137–2147.
17. Fuchs R, Male P, Mellman I. Acidification and ion permeabilities of highly purified rat liver endosomes. J Biol Chem 1989;264: 2212–2220.
18. Van Dyke RW. Proton pump-generated electrochemical gradients in rat liver multivesicular bodies. Quantitation and effects of chloride. J Biol Chem 1988;263: 2603–2611.
19. D'Souza S, Garcia-Cabado A, Yu F, Teter K, Lukacs G, Skorecki K, Moore HP, Orlowski J, Grinstein S. The epithelial sodium-hydrogen antiporter Na+/H+ exchanger 3 accumulates and is functional in recycling endosomes. J Biol Chem 1998;273: 2035–2043.
20. Bomsel M, Prydz K, Parton RG, Gruenberg J, Simons K. Endocytosis in filter-grown Madin–Darby canine kidney cells. J Cell Biol 1989;109: 3243–3258.
21. Parton RG, Prydz K, Bomsel M, Simons K, Griffiths G. Meeting of the apical and basolateral endocytic pathways of the Madin–Darby canine kidney cell in late endosomes. J Cell Biol 1989;109: 3259–3272.
22. Apodaca G, Katz LA, Mostov KE. Receptor-mediated transcytosis of IgA in MDCK cells is via apical recycling endosomes. J Cell Biol 1994;125: 67–86.
23. Barroso M, Sztul ES. Basolateral to apical transcytosis in polarized cells is indirect and involves BFA and trimeric G protein sensitive passage through the apical endosome. J Cell Biol 1994;124: 83–100.
24. Futter CE, Gibson A, Allchin EH, Maxwell S, Ruddock LJ, Odorizzi G, Domingo D, Trowbridge IS, Hopkins CR. In polarized MDCK cells basolateral vesicles arise from clathrin-gamma-adaptin-coated domains on endosomal tubules. J Cell Biol 1998;132: 611–624.

25. Odorizzi G, Pearse A, Domingo D, Trowbridge IS, Hopkins CR. Apical and basolateral endosomes of MDCK cells are interconnected and contain a polarized sorting mechanism. J Cell Biol 1996;135: 139–152.
26. Henkel JR, Apodaca G, Altschuler Y, Hardy S, Weisz OA. Selective perturbation of apical membrane traffic by expression of influenza M2, an acid-activated ion channel, in polarized Madin–Darby canine kidney cells. Mol Biol Cell 1998;9: 2477–2490.
27. Shi LB, Fushimi K, Bae HR, Verkman AS. Heterogeneity in ATP-dependent acidification in endocytic vesicles from kidney proximal tubule. Measurement of pH in individual endocytic vesicles in a cell-free system. Biophys J 1991;59: 1208–1217.
28. Van Dyke RW. Acidification of rat liver lysosomes: quantitation and comparison with endosomes. Am J Physiol 1993;265: C901–C917.
29. Van Dyke RW, Belcher JD. Acidification of three types of liver endocytic vesicles: similarities and differences. Am J Physiol 1994;266: C81–C94.
30. Dunn KW, Park J, Semrad CE, Gelman DL, Shevell T, McGraw TE. Regulation of endocytic trafficking and acidification are independent of the cystic fibrosis transmembrane regulator. J Biol Chem 1994;269: 5336–5345.
31. Gekle M, Mildenberger S, Freudinger R, Silbernagl S. Endosomal alkalinization reduces J_{max} and K_m of albumin receptor-mediated endocytosis in OK cells. Am J Physiol 1995;268: F899–F906.
32. Breitfeld PP, Casanova JE, Harris JM, Simister NE, Mostov KE. Expression and analysis of the polymeric immunoglobulin receptor in Madin–Darby canine kidney cells using retroviral vectors. Methods Cell Biol 1989;32: 329–337.
33. Brown PS, Wang E, Aroeti B, Chapin SJ, Mostov KE, Dunn KW. Definition of distinct compartments in polarized Madin–Darby canine kidney (MDCK) cells for membrane-volume sorting, polarized sorting and apical recycling. Traffic 2000;1: 124–140.
34. Dunn KW, Mayor S, Myers JN, Maxfield FR. Applications of ratio fluorescence microscopy in the study of cell physiology. FASEB J 1994;8: 573–582.
35. Presley JF, Mayor S, McGraw TE, Dunn KW, Maxfield FR. Bafilomycin A1 treatment retards transferrin receptor recycling more than bulk membrane recycling. J Biol Chem 1997;272: 13929–13936.
36. Teter K, Chandy G, Quinones B, Pereyra K, Machen T, Moore HP. Cellubrevin-targeted fluorescence uncovers heterogeneity in the recycling endosomes. J Biol Chem 1998;273: 19625–19633.
37. Sipe DM, Murphy RF. High-resolution kinetics of transferrin acidification in BALB/c 3T3 cells: exposure to pH 6 followed by temperature-sensitive alkalinization during recycling. Proc Natl Acad Sci USA 1987;84: 7119–7123.
38. Yamashiro DJ, Tycko B, Fluss SR, Maxfield FR. Segregation of transferrin to a mildly acidic (pH 6.5) para-Golgi compartment in the recycling pathway. Cell 1984;37: 789–800.
39. Hughson EJ, Hopkins CR. Endocytic pathways in polarized Caco-2 cells: identification of an endosomal compartment accessible from both apical and basolateral surfaces. J Cell Biol 1990;110: 337–348.
40. Knight A, Hughson E, Hopkins CR, Cutler DF. Membrane protein trafficking through the common apical endosome compartment of polarized Caco-2 cells. Mol Biol Cell 1995;6: 597–610.
41. Bomsel M, Parton R, Kuznetsov SA, Schroer TA, Gruenberg J. Microtubule- and motor-dependent fusion *in vitro* between apical and basolateral endocytic vesicles from MDCK cells. Cell 1990;62: 719–731.
42. Dunn KW, McGraw TE, Maxfield FR. Iterative fractionation of recycling receptors from lysosomally destined ligands in an early sorting endosome. J Cell Biol 1989;109: 3303–3314.
43. Mayor S, Presley JF, Maxfield FR. Sorting of membrane components from endosomes and subsequent recycling to the cell surface occurs by a bulk flow process. J Cell Biol 1993;121: 1257–1269.
44. Stoorvogel W, Geuze HJ, Strous GJ. Sorting of endocytosed transferrin and asialoglycoprotein occurs immediately after internalization in HepG2 cells. J Cell Biol 1987;104: 1261–1268.
45. Lang F, Paulmichl M. Properties and regulation of ion channels in MDCK cells. Kidney Int 1995;48: 1200–1205.
46. Aniento F, Gu F, Parton RG, Gruenberg J. An endosomal beta COP is involved in the pH-dependent formation of transport vesicles destined for late endosomes. J Cell Biol 1996;133: 29–41.
47. Henkel JR, Popovich JL, Gibson GA, Watkins SC, Weisz OA. Selective perturbation of early endosome and/or *trans*-Golgi network pH but not lysosome pH by dose-dependent expression of influenza M2 protein. J Biol Chem 1999;274: 9854–9860.
48. Calhoun BC, Lapierre LA, Chew CS, Goldenring JR. Rab11a redistributes to apical secretory canaliculus during stimulation of gastric parietal cells. Am J Physiol 1998;275: C163–C170.
49. Cardone MH, Smith BL, Song W, Mochly-Rosen D, Mostov KE. Phorbol myristate acetate-mediated stimulation of transcytosis and apical recycling in MDCK cells. J Cell Biol 1994;124: 717–727.
50. Presley JF, Mayor S, Dunn KW, Johnson LS, McGraw TE, Maxfield FR. The End2 mutation in CHO cells slows the exit of transferrin receptors from the recycling compartment but bulk membrane recycling is unaffected. J Cell Biol 1993;122: 1231–1241.
51. Casanova JE, Wang X, Kumar R, Bhartur SG, Navarre J, Woodrum JE, Altschuler Y, Ray GS, Goldenring JR. Association of Rab25 and Rab11a with the apical recycling system of polarized Madin–Darby canine kidney cells. Mol Biol Cell 1999;10: 47–61.
52. Goldenring JR, Soroka CJ, Shen KR, Tang LH, Rodriguez W, Vaughan HD, Stoch SA, Modlin IM. Enrichment of rab11, a small GTP-binding protein, in gastric parietal cells. Am J Physiol 1994;267: G187–G194.
53. Green EG, Ramm E, Riley NM, Spiro DJ, Goldenring JR, Wessling R. Rab11 is associated with transferrin-containing recycling compartments in K562 cells. Biochem Biophys Res Commun 1997;239: 612–616.
54. Hunziker W, Peters PJ. Rab17 localizes to recycling endosomes and regulates receptor-mediated transcytosis in epithelial cells. J Biol Chem 1998;273: 15734–15741.
55. Moore RH, Tuffaha A, Millman EE, Dai W, Hall HS, Dickey BF, Knoll BJ. Agonist-induced sorting of human beta2-adrenergic receptors to lysosomes during downregulation. J Cell Sci 1999;112: 329–338.
56. Ren M, Xu G, Zeng J, De Lemos-Chiarandini C, Adesnik M, Sabatini DD. Hydrolysis of GTP on rab11 is required for the direct delivery of transferrin from the pericentriolar recycling compartment to the cell surface but not from sorting endosomes. Proc Natl Acad Sci USA 1998;95: 6187–6192.
57. Ullrich O, Reinsch S, Urbe S, Zerial M, Parton RG. Rab11 regulates recycling through the pericentriolar recycling endosome. J Cell Biol 1996;135: 913–924.
58. van IJzendoorn SC, Hoekstra D. (Glyco)sphingolipids are sorted in sub-apical compartments in HepG2 cells: a role for non-Golgi-related intracellular sites in the polarized distribution of (glyco)sphingolipids. J Cell Biol 1998;142: 683–696.
59. van IJzendoorn SC, Hoekstra D. The subapical compartment: a novel sorting centre? Trends Cell Biol 1999;9: 144–149.
60. Zacchi P, Stenmark H, Parton RG, Orioli D, Lim F, Giner A, Mellman I, Zerial M, Murphy C. Rab17 regulates membrane trafficking through apical recycling endosomes in polarized epithelial cells. J Cell Biol 1998;140: 1039–1053.
61. Pitas RE, Innerarity TL, Weinstein JN, Mahley RW. Acetoacetylated lipoproteins used to distinguish fibroblasts from macrophages *in vitro* by fluorescence microscopy. Arteriosclerosis 1981;1: 177–185.
62. Maxfield FR, Dunn KW. In Herman B, Jacobsen K (Eds.), Studies of Endocytosis Using Image Intensification Fluorescence Microscopy and Digital Image Analysis. New York: Alan R. Liss, 1990: 357–371.
63. Dunn KW, Maxfield FR. Ratio imaging instrumentation. Methods Cell Biol 1998;56: 217–236.